MOLECULAR AND CELLULAR BIOLOGY, May 1997, p. 2876–2887 Vol. 17, No. 5
0270-7306/97/$04.00+0
Copyright © 1997, American Society for Microbiology

DNA Binding by MADS-Box Transcription Factors: a Molecular Mechanism for Differential DNA Bending

ADAM G. WEST, PAUL SHORE,† AND ANDREW D. SHARROCKS*

Department of Biochemistry and Genetics, Medical School, University of Newcastle upon Tyne, Newcastle upon Tyne, NE2 4HH, United Kingdom

Received 6 December 1996/Returned for modification 31 January 1997/Accepted 25 February 1997

The serum response factor (SRF) and myocyte enhancer factor 2A (MEF2A) represent two human members of the MADS-box transcription factor family. Each protein has a distinct biological function which is reflected by the distinct specificities of the proteins for coregulatory protein partners and DNA-binding sites. In this study, we have investigated the mechanism of DNA binding utilized by these two related transcription factors. Although SRF and MEF2A belong to the same family and contain related DNA-binding domains, their DNA-binding mechanisms differ in several key aspects. In contrast to the dramatic DNA bending induced by SRF, MEF2A induces minimal DNA distortion. A combination of loss- and gain-of-function mutagenesis identified a single amino acid residue located at the N terminus of the recognition helices as the critical mediator of this differential DNA bending. This residue is also involved in determining DNA-binding specificity, thus indicating a link between DNA bending and DNA-binding specificity determination. Furthermore, different basic residues within the putative recognition α-helices are critical for DNA binding, and the role of the C-terminal extensions to the MADS box in dimerization between SRF and MEF2A also differs. These important differences in the molecular interactions of SRF and MEF2A are likely to contribute to their differing roles in the regulation of specific gene transcription.

The MADS-box transcription factor family (MCM1, AG, DEFA, and serum response factor [SRF]) is comprised of more than 40 proteins from a variety of eukaryotic organisms ranging from yeasts to humans (reviewed in reference 34). MADS-box transcription factors play key roles in controlling diverse biological processes such as floral organ development (reviewed in references 16 and 36) and yeast cell-type-specific gene transcription (reviewed in reference 6). In humans, the MADS-box transcription factor SRF regulates immediate-early gene expression (reviewed in reference 35), whereas myocyte enhancer factor 2 (MEF2) proteins have been implicated in regulating mammalian muscle-specific gene regulation (reviewed in reference 2). To date, four genes encoding MEF2 proteins have been identified (designated MEF2A to -D [1]).

MADS-box proteins contain minimal core DNA-binding domains which are comprised of an N-terminal MADS box (56 amino acids) and a C-terminal extension (≈30 amino acids) which is essential for efficient DNA binding (reviewed in reference 34). In the case of SRF, this core DNA-binding domain is sufficient to specifically bind DNA and interact with other transcription factors (reviewed in reference 34). SRF and MEF2A exhibit different DNA-binding specificities. Site selection studies have identified the consensus sequences $CC(A/T)_6GG$ and $CTA(A/T)_4TAG$ for SRF and MEF2A, respectively (22, 23). Residues located both within and N-terminal to the MADS box dictate this differential DNA-binding specificity (20, 30).

X-ray crystallography studies indicate that the dimeric SRF core DNA-binding domain ($core^{SRF}$) represents a novel structural motif (21). Three major regions of the SRF DNA-binding domain comprise its dimerization interface (21). Two of the regions, the C-terminal ends of the DNA-binding α-helix and the hydrophobic β-sheets, are located within the MADS box. The third part of the dimerization interface is located C terminally to the MADS box and consists of one α-helix from each monomer. This C-terminal extension is known as the SAM domain due to sequence similarities with the analogous domains of Arg80 and MCM1 (34). MEF2 subfamily members all contain a different conserved C-terminal extension that is known as the MEF2 domain. SRF and MEF2A are unable to form heterodimers, suggesting that they utilize different dimerization interfaces which specify heterodimerization partners (23). DNA binding is mediated mainly by an α-helix from each monomer and residues located at the N terminus of the MADS box. Mutagenic studies of SRF are consistent with these structural predictions (29). Furthermore, a mutagenic study of MEF2C indicates that this protein binds DNA in a manner similar to that of SRF, although several differences in their DNA-binding and dimerization properties were detected (18). Significant DNA bending is observed in the $core^{SRF}$-serum response element (SRE) complex (21), which is consistent with data obtained from biochemical studies (8, 31). DNA bending by SRF may play a key role in its interactions with other transcription factors, the determination of promoter architecture, or alternatively as a component of DNA recognition. Indeed, it has been proposed that DNA bending constitutes part of the binding specificity of SRF (21, 31). However, DNA bending by other MADS-box proteins has not been investigated in detail, although the high degree of sequence similarity exhibited by MADS-box transcription factors suggests that family members exhibit similar structural and DNA-binding properties.

In this study, we have investigated the DNA-binding mechanisms utilized by the MADS-box transcription factors SRF and MEF2A. Despite their strong sequence similarity, SRF and MEF2A bind DNA via different mechanisms. In contrast to the dramatic DNA bending exhibited by SRF, MEF2A mediates minimal DNA distortion. A detailed molecular analysis of this phenomenon revealed that a single amino acid residue modulates DNA bending. This residue was mapped to the N-terminal end of the recognition helices of SRF-MEF2A

* Corresponding author. Phone: 44-191 222 8800. Fax: 44-191 222 7424. E-mail: a.d.sharrocks@ncl.ac.uk.

† Present address: The Walter and Eliza Hall Institute of Medical Research, Royal Melbourne Hospital, Melbourne, Victoria 3050, Australia.

and is also involved in determining DNA-binding specificity. A possible link between DNA bending and DNA-binding specificity determination is therefore established. Moreover, different residues in SRF and MEF2A play critical roles in DNA binding, and the C-terminal extensions to the MADS box play different roles in mediating dimerization, further emphasizing the divergence in their DNA-binding mechanisms.

MATERIALS AND METHODS

Plasmid constructions and mutagenesis. The pBS-KS$^+$-derived plasmids pAS1 (encoding core^{SRF} [amino acids 132 to 222]), pAS7 (encoding core^{SRF} R157K), pAS18 (encoding core^{SRF} R164K) (29), pAS37 (encoding the truncated core^{SRF} derivative METcore^{SRF} [amino acids 142 to 222]), pAS47 (encoding METcore^{SRF} K154E) (30), pAS52 (encoding METcore^{SRF} V144K/K154E) (30), pAS53 (encoding METcore^{SRF} V144K) (30), pAS68 (encoding core^{MEF2A} [amino acids 1 to 86]) (33), pT7C4 (encoding full-length MEF2A) (23), and pAS247 (encoding Ncore^{SRF} [SRF residues 1 to 222]) have been described previously (32).

pAS135 (encoding core^{MEF2A} R17K), pAS307 (encoding core^{MEF2A} K4V/E14K), pAS308 (encoding core^{MEF2A} K4V), pAS322 (encoding core^{MEF2A} R17A), and pAS334 (encoding METcore^{SRF} H193A) were constructed with fragments obtained from a two-step PCR protocol as described previously (33) with two flanking primers (FOR and REVL) and the mutagenic primers ADS140, ADS314, ADS297, ADS181, and ADS317, respectively. PCR products were cleaved with *Nco*I and *Bam*HI and ligated into pAS37 cleaved with the same enzymes.

To produce pAS324 and pAS325, the primers MET1 and FOR (30) were used in PCRs with the templates pAS7 and pAS18. The resulting products were cleaved with *Nco*I and *Bam*HI and ligated into pAS37 cleaved with these enzymes to produce pAS324 (encoding METcore^{SRF} R157K) and pAS325 (encoding METcore^{SRF} R164K), respectively. To produce pAS244 (encoding SRF:MEF [SRF residues 131 to 197 fused to MEF2A residues 58 to 86]), the primers ADS207 and REVL were used in a PCR with the template pAS1. The resulting product was cleaved with *Hin*dIII and *Nhe*I and ligated into pAS68 cleaved with these enzymes. pAS195 (encoding MEF:SRF [MEF2A residues 1 to 57 fused to SRF residues 198 to 222]) was constructed with fragments obtained from a two-step PCR protocol with two flanking primers (FOR and REVL) and the primer ADS198. The first step was carried out on the template pAS68, whereas the second step was carried out on the template pAS1. PCR products were cleaved with *Hin*dIII and *Bam*HI and ligated into pAS37 cleaved with these enzymes. pAS246 (encoding MEF:ZIP [MEF2A residues 1 to 58 fused to E4BP4 residues 92 to 136]) was constructed by the introduction of *Nhe*I and *Bam*HI sites into the sequence encoding the leucine zipper domain of E4BP4 (3) with the mutagenic primers ADS208 and ADS209, followed by subsequent ligation into pAS68 cleaved with these enzymes. pAS408 (encoding SRF:ZIP [SRF residues 131 to 197 fused to E4BP4 residues 92 to 136]) was constructed by removal of the *Nhe*I-*Bam*HI fragment of pAS246 and subsequent ligation into pAS244 cleaved with these enzymes. To construct pAS411 and pAS412, primers ADS338 and FOR were used in PCRs with the templates pAS246 and pAS408. The resulting products were cleaved with *Sal*I and *Bam*HI and ligated into the same sites of pAS246 and pAS408, respectively, to produce pAS411 (encoding MEF:ZIP L101R) and pAS412 (encoding SRF:ZIP L101R).

pAS409 (encoding SRF:FLI [SRF residues 131 to 197 fused to zebra fish Fli-1 residues 275 to 372]) and pAS410 (encoding MEF:FLI [MEF2A residues 1 to 58 fused to zebra fish Fli-1 residues 275 to 372]) were constructed by removal of the *Sal*I-*Bam*HI fragment of pAS302 and ligation into pAS408 and pAS246, respectively. pAS302 contains zebra fish Fli-1 219-372 (1a).

Random mutagenesis of residues in the MEF2A α-helix (residues N16 to R24) was carried out by a modification of the two-step, single-mutagenic-primer PCR protocol (15). The mutagenic oligonucleotide ADS127, which spanned amino acids Asn16 to Arg24 of MEF2A (corresponding to the N-terminal end of the putative DNA-binding α-helix), was designed. This oligonucleotide was synthesized with doped nucleotide mixes in order to generate a degenerate pool of sequences. Nucleotide mixes were contaminated with the other four nucleotides according to the formula $P(x) = [N!\{x!(N-x)!\}]\, C_m^{\,x}(1-C_m)^{N-x}$, where $P(x)$ is the probability of x mutations in an oligonucleotide containing N nucleotides and C_m is the total fractional concentration of contaminating nucleotides (5). The level of contamination was set to maximize the number of single-point mutations, where $C_m = 1/N$ (in this case, 3.4%). The following resulting mutant MEF2A proteins were produced: Q18K (pAAA22), T20L (pAAA32), K23R (pAAA24), K23N (pAAA30), R244 (pAAA43), K25T (pAAA21), K25M (pAAA34), and K25R (pAAA3).

pAS58 (encoding glutathione *S*-transferase [GST]:core^{SRF}) has been described previously (33). In the construction of pAS70 and pAS475, the primer pairs ADS101-ADS103 and ADS104-REVL were used in PCRs on the templates pAS68 and pAS37, respectively. The resulting products were cleaved with *Nco*I and *Sal*I and ligated into pET21d (Novagen) which had been cleaved with *Nco*I and *Xho*I. The resulting bacterial expression plasmids (pAS70 and pAS475) encode core^{MEF2A} (amino acids 1 to 86) and METcore^{SRF} (amino acids 142 to 222) fused to a C-terminal hexahistidine tag.

The plasmid pAS152 was constructed by ligating the two annealed phosphorylated oligonucleotides ADS165 (5′-CTAGGAGGAAAACTATTTATAGATCAAAT-3′) and ADS166 (5′-CTAGATTTGATCTATAAATAGTTTTCCTC-3′) into the *Xba*I site of pBEND2 (13). These oligonucleotides contain the MEF2A binding site N10 (underlined) (23). pAS76 is an analogous construct based on pBEND2 but instead contains the c-*fos* SRE (central sequence, 5′-CCATATTAGG-3′) (31). The plasmids pAS469 to pAS474 were constructed by ligating the two annealed phosphorylated oligonucleotides ADS339 (5′-AATTAGGAAAACTATTTATAGATCAAATGAGCT-3′) and ADS340 (5′-CATTTGATCTATAAATAGTTTTCCT-3′) into the phasing vectors SB12, -14, -16, -18, and -20 (7) that had been cleaved with *Eco*RI and *Sac*I. These oligonucleotides contain the MEF2A binding site N10 (underlined) with overhangs that permit *Eco*RI/*Sac*I cloning while destroying the *Eco*RI recognition site.

Details of mutagenic oligonucleotides can be supplied upon request.

The sequences of all plasmids encoding mutant proteins and PCR-derived sequences were confirmed by automated and manual dideoxy sequencing.

Protein production. Wild-type and mutant SRF and MEF2A proteins were produced by either sequential transcription and translation from linearized plasmid DNA or by coupled transcription-translation with TNT rabbit reticulocyte lysates on closed circular templates (Promega). ^{35}S-labelled proteins were routinely analyzed by electrophoresis through 0.1% sodium dodecyl sulfate–12% polyacrylamide gels before visualization, and bands representing intact proteins were quantified by phosphorimaging (Fuji BAS-1500 phosphorimager and TINA 2.08e software).

SRF and MEF2A derivatives were also purified from overexpressing *Escherichia coli* strains. core^{SRF} was purified from *E. coli* GM119 which had been transformed with pAS58 as described previously (33). core^{MEF2A} and METcore^{SRF} were expressed in the *E. coli* strain BL21(DE3)pLysS transformed with pAS70 and pAS475, respectively, and purified by single-step nickel-affinity chromatography according to the Novagen protocol.

Gel retardation and circular permutation analysis. Gel retardation assays were carried out essentially as described previously (31) with the c-*fos* SRE (33), the N10 site (central motif, CTATTTATAG), or M1, the mutant SRE-like N10 site (central motif, CCATTTATGG) (30). Relative DNA-binding affinities were calculated by PhosphorImager analysis of DNA-protein complexes (Fuji BAS1500 and TINA 2.08e software). Experiments were carried out to achieve ≤50% of total DNA binding in protein-DNA complexes. Under these conditions, relative binding affinities within an experiment can be calculated by direct quantification of DNA-protein complexes. The scores for these relative binding affinities are indicated in the figure legends.

For circular permutation analysis, DNA fragments were produced by appropriate restriction enzyme digestion of PCR products derived from the vectors pAS76 (containing the SRE) and pAS152 (containing the N10 site) as described previously (31). All DNA-binding sites were purified from nondenaturing 10% polyacrylamide gels. Curve fitting and apparent DNA bend angles were calculated as described previously (31). Bend angles are given as the averages of three independent experiments. Standard deviations ($n - 1$) of bend angles are in the range 0.5 to 1.6°. However, in order to show direct visual comparisons of data obtained from proteins that give rise to complexes of differing mobilities, the data were normalized for the complex with the fastest mobility (11).

All figures were generated electronically from scanned images of autoradiographic images by using Picture Publisher (Micrografx) and Powerpoint (Microsoft) software. Final images are representative of the original autoradiographic images.

Ligase-mediated circularization assay. The rates of circularization of phase-sensitive probes were determined in the presence and absence of bacterially expressed METcore^{SRF} or core^{MEF2A}. The oligonucleotides ADS346 (5′-GGCTACAATGAATTCATAACCTT-3′) and ADS347 (5′-ATCGAAATGAATTCGACTCAC-3′) (*Eco*RI sites underlined) were used to produce ^{32}P-labelled DNA fragments by PCR with the N10 phasing vectors pAS469 to -474 as templates. PCR products were subsequently digested with *Eco*RI and then gel purified. The resulting probes varied from 230 to 238 bp. The 5′ and 3′ ends were 62 and 64 bp from the centers of the N10 and last A:T tract, respectively. Gel retardation analysis was used to determine firstly that linker lengths of 55 and 59 bp (center of N10 site to center of first A:T tract) caused the N10 binding site to be in and out of phase with the six A:T tracts, respectively, and secondly the quantity of METcore^{SRF} or core^{MEF2A} that gave 50% binding to each probe in the absence of competitor DNA.

Ligase-mediated circularization assays were carried out essentially as described previously (9). Proteins were preincubated with DNA probes in 50 μl under gel retardation buffer conditions (2 mM spermidine, 60 mM KCl, 8 mM HEPES [pH 7.9], 6.4% glycerol, 0.64 mM $MgCl_2$, 0.32 mM dithiothreitol [DTT], 0.032 μM $ZnCl_2$) for 20 min at 22°C and then placed on ice. Ligation reactions were initiated by the addition of an equal volume of 10 mM $MgCl_2$–4 mM ATP–2 mM DTT–0.02% Nonidet P-40–2 mM spermidine–8 mM HEPES (pH 7.9)–6.4% glycerol–0.032 μM $ZnCl_2$–80 μg of bovine serum albumin per ml–T4 DNA ligase (MBI Fermentas). The final concentration of DNA ligase varied from 10 to 100 U/ml, and all reactions were carried out at 4°C. Each phasing probe tested recircularized at a different rate in the absence of added binding protein. Samples (10 μl) were taken between 0 and 60 min and quenched with 5 μl of 75 mM EDTA–2 mg of proteinase K per ml–15% glycerol containing 0.2% xylene cyanol–0.2% bromophenol blue. Quenched samples were incubated at 55°C for 15 min immediately prior to loading on prerun 5% acrylamide–1× Tris-borate-EDTA gels at 200 V. A second sample was taken after 60 min and incubated at

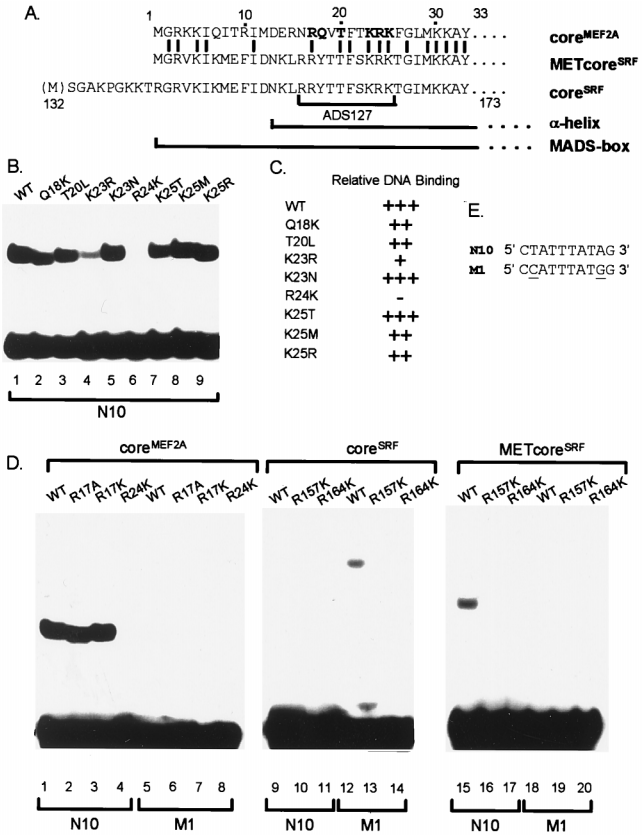

FIG. 1. Different basic residues play critical roles in DNA binding by SRF and MEF2A. (A) Sequences of the N-terminal ends of the core^{MEF}, core^{SRF}, and METcore^{SRF} DNA-binding domains. The numbers above and below these sequences refer to MEF2A and SRF amino acid residues, respectively. Residues within the MADS box, recognition α-helix, and the mutagenic oligonucleotide are bracketed. Residues targeted by mutagenesis of MEF2A are shown in boldface. (B) Gel retardation analysis of mutant MEF2A proteins to the N10 binding site. Equal molar quantities of each protein were used in DNA binding reactions. (C) Summary of binding of mutant proteins relative to wild-type MEF2A. +++, >65%; ++, 10 to 65%; +, 1 to 10%; −, not detectable. (D) Gel retardation analysis of wild-type and mutant MEF2A, SRF, and METSRF core DNA-binding domains to the N10 and M1 binding sites. (E) Sequences of the central 10-bp motifs of the N10 and M1 binding sites. Residues mutated in the N10 site to create the M1 site are underlined. WT, wild type.

65°C for 10 min, followed by digestion with 1.6 U of exonuclease III (Gibco/BRL) at 37°C for 30 min, prior to quenching and loading to remove single-stranded DNA and to identify circular reaction products.

RESULTS

Identification of amino acids that play distinct roles in DNA binding by SRF and MEF2A. To investigate potential differences in DNA-binding mechanisms, we firstly determined which amino acids play essential roles in DNA binding in MEF2A. The majority of DNA contacts made by SRF are made by residues located in a recognition α-helix (21). Three basic residues, R157, K163, and R164, play essential roles in DNA binding (29). Further residues in the N-terminal end of the recognition α-helix and the N-terminal tail play roles in modulating the binding specificity of SRF (20, 30). MEF2A shows strong sequence identity with SRF throughout the recognition helix, with the greatest identity toward the C-terminal end of the α-helix (Fig. 1A). This suggests that MEF2A will also use an α-helix to bind to DNA. To test this prediction and to identify amino acids in MEF2A which play critical roles in DNA binding, a mutagenic approach was adopted. Firstly, random mutagenesis was used to assess the roles of individual amino acids at the N-terminal end of the recognition helix. Mutations were created in the minimal core DNA-binding domain of MEF2A (amino acids 1 to 86) and compared to similar core domain derivatives of SRF for binding to the N10 and M1 binding sites. The N10 site is bound with high affinity by MEF2A, whereas the M1 site differs at two positions and resembles the SRF binding site in the c-*fos* SRE (23, 30) (Fig. 1E). Therefore, the M1 site represents a good binding site for SRF but is bound by MEF2A with low affinity (23). The core domain of MEF2A retains high-affinity sequence-specific DNA binding (28) (Fig. 1D, lanes 1 and 5). Mutations in five different residues in core^{MEF2A} were detected. All of the proteins containing these mutations bound DNA efficiently, with the exception of MEF2A (K23R) (Fig. 1B, lane 4), which bound with reduced efficiency, and MEF2A (R24K) (Fig. 1B, lane 6), which bound DNA with negligible affinity. Site-directed mutagenesis was used to investigate the role of an additional basic residue in MEF2A (R17) which was not targeted by the random approach. Both MEF2A (R17A) and MEF2A (R17K) bound DNA efficiently (Fig. 1D, lanes 2 and 3). In contrast, the SRF protein containing the analogous mutation (R157K) bound DNA with negligible affinity (Fig. 1D, lane 13), thereby indicating a different role for this residue in MEF2A and SRF. However, in common with MEF2A, the mutation of the basic residues K163 (29) and R164 in SRF (analogous to K23 and R24 in MEF2A) also reduced DNA binding (29) (Fig. 1D).

The role of R157 in the mutant SRF protein METcore^{SRF}, which exhibits a DNA-binding specificity similar to that of MEF2A (20, 30) (Fig. 1D, lanes 12 and 15), was also investigated. However, in contrast to MEF2A (R17K), METcore^{SRF} (R157K) is unable to bind DNA efficiently, which further demonstrates the differential role of this residue in mediating DNA binding.

A recent targeted mutagenic study of the highly related protein MEF2C also identified R23 and R24 as critical DNA-binding determinants, whereas R17 was shown to play a less-important role in DNA binding (18). The present study of MEF2A uses more conservative substitutions (alanine and arginine/lysine) at the equivalent positions to demonstrate a similar role for these residues and further demonstrates that other residues in the putative recognition helix are not critical for DNA binding. Taken together, these results demonstrate that although similarities in how SRF and members of the MEF2 family bind to DNA exist, the two proteins clearly bind DNA in different ways. The basic residues R17 and R157 are located in identical positions in the MADS box and yet play distinct roles in the two proteins. In MEF2, R17 appears unimportant, whereas in SRF, R157 is essential for efficient DNA binding.

Dimerization of SRF and MEF2A. An intact C-terminal extension to the MADS box is required for efficient DNA binding and dimerization of SRF and MEF2A (19, 23). However, SRF and MEF2A are unable to form heterodimers, suggesting that they utilize different dimerization interfaces (23) (Fig. 2D, lanes 13 to 16, and C, lanes 13 to 16).

In order to assess the roles of the MADS box and C-terminal extensions in mediating this dimerization specificity, chimeric proteins were constructed by exchanging the MADS boxes of MEF2A and SRF (Fig. 2A). The resulting chimeras, SRF:MEF and MEF:SRF, specifically bound to the SRE and N10 sites, respectively (Fig. 2B), thereby demonstrating that the MADS boxes are sufficient to mediate the correct DNA-binding specificities of these transcription factors. Furthermore, since both chimeras bind DNA (albeit weakly in the case of the SRF:MEF chimera), this demonstrates that both chimeras

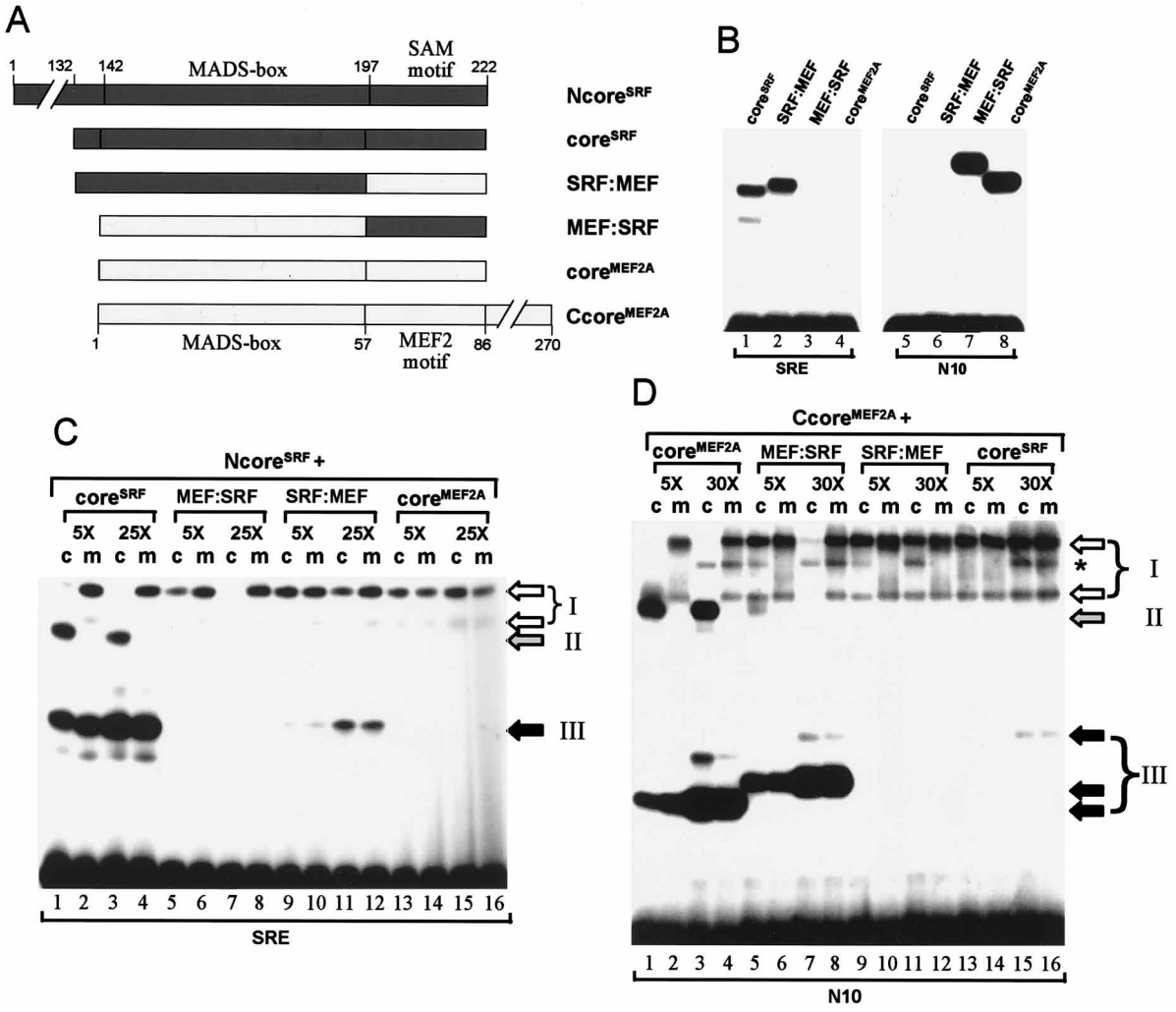

FIG. 2. Dimerization determinants of SRF and MEF2A. (A) Diagrammatic representation of truncated and chimeric SRF and MEF2A proteins. The numbers indicate the positions of SRF- or MEF2A-derived residues with respect to the full-length proteins. SRF- and MEF2A-derived sequences are indicated by darkly and lightly shaded boxes, respectively. (B) Gel retardation analysis of wild-type and chimeric SRF and MEF2A proteins binding to the c-*fos* SRE and N10 sites. In order to demonstrate the specificity of binding, the quantities of proteins added were adjusted to produce equal-intensity complexes in lanes 1 and 2 and lanes 7 and 8. Equal molar quantities of core^{MEF2A} and MEF:SRF were used. Due to the lower affinity of SRF:MEF for the SRE, a 20:1 ratio of SRF:MEF to core^{SRF} was used. (C and D). Heterodimerization of wild-type and chimeric SRF and MEF2A proteins. Gel retardation analysis of complexes formed between Ncore^{SRF} and the SRE (C) or between Ccore^{MEF2A} and the N10 site (D) and wild-type and chimeric core^{SRF} and core^{MEF2A} derivatives. Proteins were either cotranslated (c) or mixed after translation (m). Open arrows (I), complexes formed by Ncore^{SRF} and Ccore^{MEF2A} (long-form) homodimers; closed arrows (III), complexes formed by core^{SRF}, core^{MEF2A}, SRF:MEF, and MEF:SRF (short form). Ncore^{SRF} and Ccore^{MEF2A} homodimers give rise to a major complex and to a second lower-mobility complex. The positions of complexes containing heterodimers are indicated by shaded arrows (II). Asterisk, a complex formed on the N10 site by proteins in the rabbit reticulocyte lysate. 5×, 25×, and 30×, ratios of short-form to long-form proteins (5:1, 25:1, and 30:1, respectively).

dimerize and suggests that the MADS boxes and C-terminal extensions act as cooperative, independent dimerization motifs.

To further investigate the roles of the MADS box and C-terminal extensions in mediating dimerization, the chimeric proteins were tested for their abilities to dimerize with wild-type SRF or MEF2A derivatives. Minimal DNA-binding domains were cotranslated with longer SRF (Ncore^{SRF}) or MEF2A (Ccore^{MEF2A}) proteins (Fig. 2A), and their abilities to form heterodimers were assessed either by the formation of a DNA-bound complex with intermediate mobilities or alternatively by recruitment of the wild-type proteins into an inactive non-DNA binding heterodimer (19). core^{SRF} and core^{MEF2A} form DNA-binding heterodimers of intermediate mobilities with the longer Ncore^{SRF} and Ccore^{MEF2A} proteins, respectively (Fig. 2C, lanes 1 to 4, and D, lanes 1 to 4). Cotranslation is essential for the formation of such heterodimers (19, 23) (Fig. 2C and D [compare lanes c and m]). In contrast, neither core^{SRF} (Fig. 2D, lanes 13 to 16) nor core^{MEF2A} (Fig. 2C, lanes 13 to 16) forms heterodimers with the reciprocal longer-form proteins, indicating that specificity determinants of dimerization exist. In order to determine the relative contributions of the MADS boxes and C-terminal extensions in determining dimerization specificity, the chimeric proteins MEF:SRF and SRF:MEF were tested for dimerization with the wild-type proteins. MEF:SRF forms non-DNA-binding heterodimers with Ncore^{SRF} (Fig. 2C, lanes 5 to 8), whereas SRF:MEF forms heterodimers weakly with Ncore^{SRF} (Fig. 2C, lanes 9 to 12; visible on longer exposure). This indicates that the C-terminal SAM domain of MEF:SRF is the major dimerization determinant in SRF. A similar pattern is observed with dimerization of

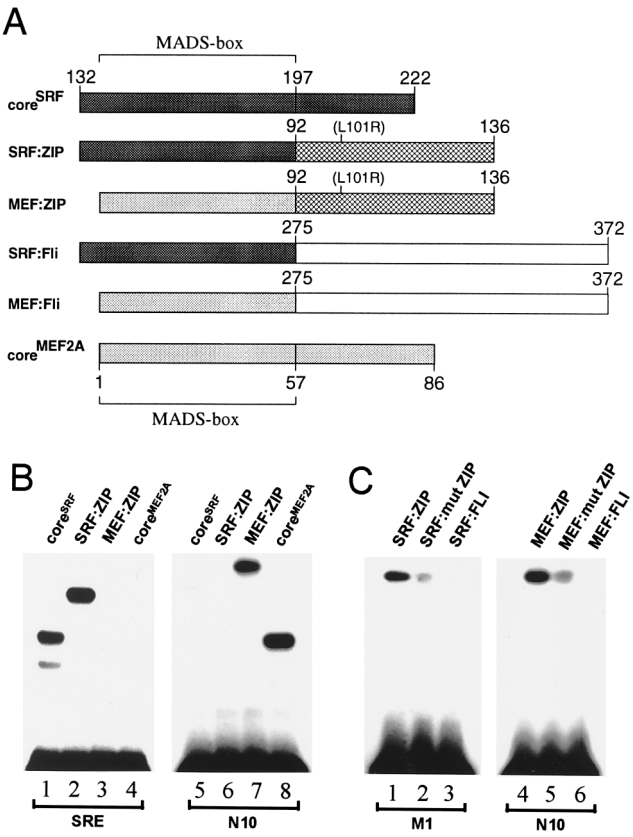

FIG. 3. The SAM and MEF2 motifs of SRF and MEF2A can be functionally replaced by an alternative dimerization motif. (A) Diagrammatic representation of chimeric SRF and MEF2A proteins. The locations of the MADS boxes are indicated. Numbers indicate the positions of SRF (darkly shaded boxes)-, MEF2A (lightly shaded boxes)-, E4BP4 (cross-hatched boxes)-, and zebra fish Fli-1 (open boxes)-derived sequences with respect to the full-length proteins. The positions of the mutation introduced into the leucine zipper of E4BP4 are indicated above the SRF:ZIP and MEF:ZIP chimeras. (B) Gel retardation analysis of wild-type and chimeric SRF and MEF2A proteins binding to the c-*fos* SRE and N10 sites. Equal quantities of each protein were used with each binding site (lanes 1 and 5, 2 and 6, 3 and 7, and 4 and 8) in order to demonstrate the specificity of binding. (C) Gel retardation analysis of wild-type and mutant SRF (lanes 1 to 3) and MEF (lanes 4 to 6) chimeras bound to the M1 and N10 binding sites. Equal quantities of SRF- and MEF2A-derived chimeric proteins were used on the M1 (lanes 1 to 3) and N10 (lanes 4 to 6) sites, respectively.

these chimeras with Ccore^{MEF2A}. MEF:SRF forms non-DNA-binding heterodimers with Ccore^{MEF2A} (Fig. 2D, lanes 5 to 8), whereas SRF:MEF forms heterodimers weakly with Ccore^{MEF2A} (Fig. 2D, lanes 9 to 12; visible on longer exposure). In contrast to SRF, this indicates that the MADS box in the MEF:SRF chimera is the major dimerization determinant in MEF2A.

These results further demonstrate that the MADS box and C-terminal extensions both contribute to dimerization. However, the MADS box and C-terminal extensions appear to play different roles in dimerization in SRF and MEF2A. The C-terminal SAM domain is the major mediator of dimerization specificity in SRF, whereas the MADS box performs a similar function in MEF2A.

To further investigate the roles of the MADS boxes in mediating dimerization of SRF and MEF2A, a further series of chimeric proteins were synthesized. The MADS boxes of SRF and MEF2A were fused to the leucine zipper dimerization domain of E4BP4 (3) or the ETS domain of zebra fish Fli-1 (1a). The latter domain is not thought to mediate dimerization (Fig. 3A). The chimeras SRF:ZIP and MEF:ZIP bound specifically to the SRE and N10 sites, respectively (Fig. 3B). This further demonstrates that the MADS boxes are sufficient to determine the DNA-binding specificities of SRF and MEF2A. Moreover, this demonstrates that the C-terminal extension can be replaced by an alternative dimerization motif, indicating that the MADS boxes are sufficient to align the DNA-binding α-helices in the absence of their natural C termini. In contrast, DNA binding by the SRF:FLI and MEF:FLI chimeras cannot be detected (Fig. 3C, lanes 3 and 6). Furthermore, mutations within the leucine zipper of the MEF:ZIP and SRF:ZIP chimeras reduce the efficiency of DNA binding, thereby demonstrating the requirement for a fully functional dimerization motif for efficient DNA binding. Therefore, these data indicate that while the MADS boxes are sufficient to align the DNA-binding α-helices and direct sequence-specific DNA binding, their C-terminal extensions or a heterologous dimerization domain is required to permit efficient DNA binding.

Differential DNA bending by SRF and MEF2A. SRF bends DNA significantly. Indeed, an excellent correlation is observed from X-ray crystallography studies and circular permutation analysis (8, 21, 31). However, since SRF and MEF2A utilize different residues as the key determinants of DNA binding and dimerization, they may also distort DNA to different extents. To test this hypothesis, we investigated the ability of MEF2A to bend DNA by the circular permutation assay.

In contrast to SRF, the core DNA-binding domain of MEF2A induced minimal distortion of its natural DNA-binding site (Fig. 4B; 73.0 ± 0.93° for core^{SRF} and 19.3 ± 1.04° for core^{MEF2A}). This differential DNA bending either may be an intrinsic property of the DNA-binding domains themselves or alternatively may be due to differences in the DNA-binding sequences recognized by each protein. Indeed, several differences exist within the sequences of the N10- and SRE-binding sites both within the central core 10 bp (see Fig. 9C) and among the flanking nucleotides. Such differences may make the N10 site refractory to protein-induced bending. SRF binds weakly to the N10-binding site (30) but, unlike MEF2A, bends this site to a degree comparable to that of the c-*fos* SRE (Fig. 4B). Moreover, a truncated core^{SRF} derivative (METcore^{SRF}) which shows an altered DNA binding specificity and preferentially binds to the N10 site (30) bends both the SRE (66.4 ± 0.77°) and the N10 (59.5 ± 1.08°) sites to similar extents (Fig. 4B). This indicates that the N-terminal 10 amino acids of core^{SRF}, which play a major role in determining its DNA-binding specificity, play minimal roles in allowing SRF to bend DNA. Taken together, these data demonstrate that the difference in the ability to induce DNA bending is not due to an inherent inability of this sequence to bend. Instead, the differential induction of DNA bending reflects an intrinsic property of the SRF and MEF2A DNA-binding domains.

In addition to protein-induced DNA bending, other factors, including protein shape, can influence the mobility of protein-DNA complexes in a circular permutation assay. Two different assays, therefore, were performed to further investigate the differential DNA bending exhibited by SRF and MEF2A. Firstly, phasing analysis was used to investigate the ability of a protein-induced bend to enhance or counteract an intrinsic bend. In agreement with a previous study of the c-*fos* SRE (31), SRF-inducible DNA bending was detected by this assay. However, little phase-sensitive deviation in probe mobility was induced by MEF2A (data not shown), further emphasizing the differential abilities of SRF and MEF2A to induce DNA bending. A second assay, ligase-mediated circularization, which was based on the results of the phasing analysis was performed. This assay has the advantage that it is solution based and does

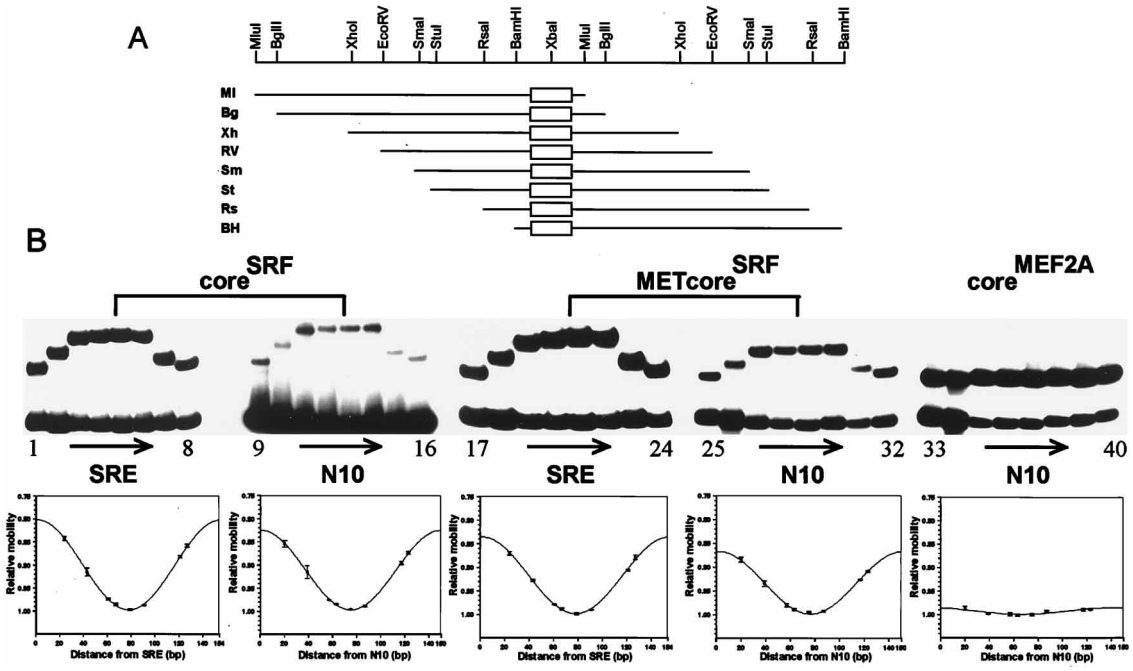

FIG. 4. SRF and MEF2A bend DNA to different extents. Circular permutation analysis of SRF and MEF2 complexes with the c-*fos* SRE and N10 site. (A) Diagrammatic representation of the SRE and N10 sites generated by restriction digestion of pAS76 and pAS152, respectively. The locations of the SRE or N10 sites are indicated by open boxes. Probes were generated by digestion with *Mlu*I (Ml), *Bgl*II (Bg), *Xho*I (Xh), *Eco*RV (EV), *Sma*I (Sm), *Stu*I (St), *Rsa*I (Rs), or *Bam*HI (BH). (B) Gel retardation analysis of core^{SRF}, METcore^{SRF}, and core^{MEF2A} bound to each of the circularly permuted probes containing either the c-*fos* SRE (lanes 1 to 8 and 17 to 24) or the N10 site (lanes 9 to 16, 25 to 32, and 33 to 40). The following probes were used: M1 (lanes 1, 9, 17, 25, and 33), Bg (lanes 2, 10, 18, 26, and 34), Xh (lanes 3, 11, 19, 27, and 35), EV (lanes 4, 12, 20, 28, and 36), Sm (lanes 5, 13, 21, 29, and 37), St (lanes 6, 14, 22, 30, and 38), Rs (lanes 7, 15, 23, 31, and 39), and BH (lanes 8, 16, 24, 32, and 40). Since core^{SRF} and METcore^{SRF} exhibit reciprocal DNA-binding specificities, 10-fold more core^{SRF} was used in binding to the N10 site and 10-fold more METcore^{SRF} was used in binding to the SRE than that in binding to each of the reciprocal sites. The data from each circular permutation experiment are shown graphically beneath each set of primary data. The relative mobilities of protein-DNA complexes were normalized for differences in probe mobilities (see Materials and Methods) and plotted as a function of the position of the center of the SRE or N10 site from the 5′ end of the probe. The points are connected by a curve of the best fit of a cosine function. The mobilities of MEF2A-N10 complexes exhibit a poor fit to the cosine function. Error bars represent standard deviations calculated from at least three independent experiments.

not rely on differences in the electrophoretic mobilities of protein-DNA complexes. In this assay, the intramolecular ligation rates of probes containing N10 sites either in or out of phase with an intrinsic DNA bend are analyzed in the presence of putative DNA-bending proteins. If protein-induced bends are introduced in the in-phase probe, then a higher ligation rate would be expected due to the increased bending and closer proximity of the two ends, whereas lower rates would be induced by binding to the out-of-phase probe. The results of the experiment are shown in Fig. 5. Probes containing the N10 site in and out of phase with an intrinsic DNA bend were selected from the phasing analysis (data not shown), and the ligase-mediated circularization rates of each probe were compared in the presence of SRF or MEF2A. In comparison to free DNA, both SRF and MEF2A inhibit ligase-mediated circularization. This general inhibition occurs in the absence of specific binding sites for the two proteins (data not shown) and probably reflects binding to the free DNA ends. The rate of ligase-mediated circularization of the in-phase probe in the presence of METcore^{SRF} was faster than that for core^{MEF2A} (Fig. 5A) as expected for SRF, which is known to induce DNA bending. In contrast, on the out-of-phase probe in which SRF-induced bending was expected to inhibit circularization, the ligase-mediated circularization rate was significantly lower for METcore^{SRF} than that for core^{MEF2A} (Fig. 5C). These data are, therefore, entirely consistent with the idea that SRF bends DNA to a greater extent than MEF2A.

Taken together, the combination of circular permutation, phasing, and ligase-mediated cyclization assays unequivocally demonstrates that SRF induces substantially more DNA bending than the highly related MEF2A.

Mapping the DNA-bending determinants of SRF and MEF2A. In order to map the residues responsible for the differential DNA bending induced by SRF and MEF2A, we first utilized several chimeric proteins containing their MADS boxes (Fig. 2A and 3A). SRF:MEF bends DNA considerably in comparison to MEF:SRF (Fig. 6; 57.4 ± 1.51° for SRF:MEF and 36.0 ± 0.59° for MEF:SRF). This suggests that the MADS boxes of SRF and MEF2A are sufficient to dictate the differential DNA bending and that the C-terminal extensions play minor roles in this process. Indeed, the SRF:ZIP and MEF:ZIP chimeras, in which the C-terminal extensions are replaced by leucine zippers, also exhibit differential DNA bending. SRF:ZIP bends DNA significantly in comparison to MEF:ZIP (Fig. 6; 64.8 ± 0.94° for SRF:ZIP and 29.4 ± 1.55° for MEF:ZIP). Since the chimeric SRF:ZIP and MEF:ZIP proteins contain highly conserved MADS boxes and identical C-terminal leucine zippers, the overall tertiary structures are unlikely to differ greatly, removing the possibility that protein shape is the reason for the differences in complex mobilities containing SRF and MEF2A derivatives. These studies with the chimeric SRF and MEF2A proteins in which these C-terminal extensions are either switched or replaced by an identical leucine zipper motif clearly demonstrate that the conserved MADS boxes are sufficient to mediate the differential DNA bending induced by these two transcription factors and that the divergent C termini play a minor role in this function.

Residues in the MADS box were subsequently mutated to

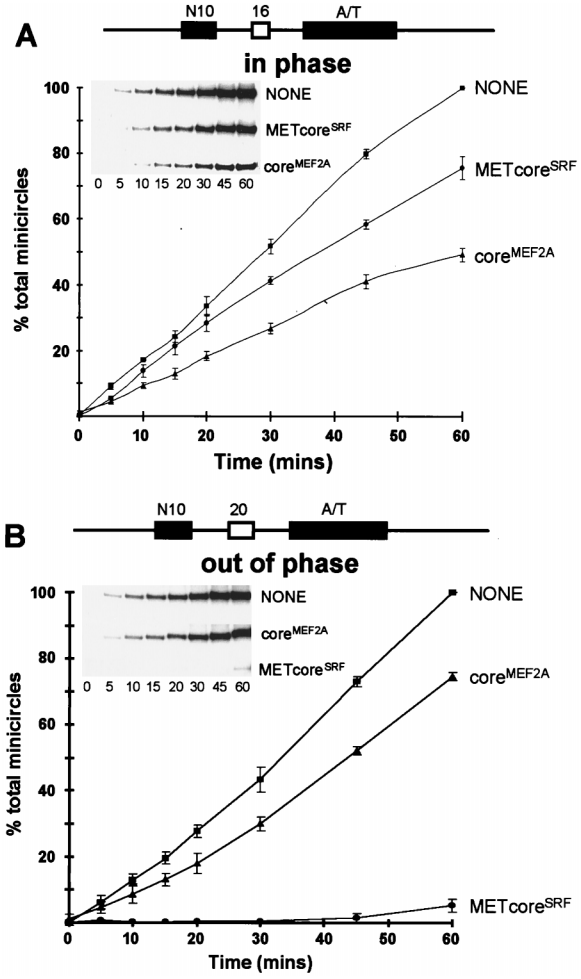

FIG. 5. SRF and MEF2A bend DNA in solution to different extents. Ligase-mediated circularization analysis of SRF and MEF2A on the N10 site is shown. Assays were carried out on sites containing linker spacers of 16 and 20 bp in which the center of the N10 site was in phase (A) or out of phase (B) with the center of a prebent poly(A:T) tract. The relative positions of the N10 site, the spacer, and the poly(A:T) tracts are shown diagrammatically. Minicircle formation after incubation with DNA ligase for the indicated times (0 to 60 min) is shown graphically. The primary data are shown as insets to the graphs. Circularization reactions were carried out in the absence (squares) or presence of $core^{MEF2A}$ (triangles) or $METcore^{SRF}$ (circles).

identify those which play a key role in DNA bending. Firstly, a loss-of-function approach was adopted in which DNA-contacting residues in SRF were exchanged for those in the analogous positions in MEF2A in order to attempt to reduce protein-induced DNA bending. Initially, several existing mutant SRF proteins were tested (30). Subsequently, following the elucidation of the structure of the SRF-DNA complex (21), other candidate residues were tested based on their involvement in contacting the DNA sugar-phosphate backbone. The introduction of the double mutation V144K/K154E into SRF severely reduces its ability to bend DNA (Fig. 7B). Moreover, in ligase-mediated circularization assays, $METcore^{SRF}$ (V144K/K154E) behaves in a manner similar to that of MEF2A (data not shown), further confirming that it exhibits significantly reduced DNA-bending ability. Of these two mutations, K154E (located at the N-terminal end of the DNA-binding α-helix; Fig. 7A) is sufficient to cause this reduction in bending, whereas in comparison, V144K plays only a minor role (Fig. 7B).

Examination of the structure of the SRF-DNA complex suggests that residues in the β-loop may play a role in contacting DNA and mediating DNA bending. The H193A mutation is predicted to disrupt such contacts and hence to disrupt SRF-induced DNA bending. Indeed, $METcore^{SRF}$ (H193A) shows reduced DNA bending, although the reduction is not as severe as that observed with $METcore^{SRF}$ (K154E) (Fig. 7B; 24.2 ± 0.9° for K154E and 49.4 ± 1.04° for H193A). The addition of the K154E mutation to $METcore^{SRF}$ (H193A) causes a further reduction in DNA bending (38). Taken together, these data indicate that residues in the β-loop region and N-terminal end of the DNA-binding α-helix contribute to DNA bending induced by SRF. However, the residues K154 (SRF) and E14 (MEF2A) appear to be the major determinants of the differential abilities of these two proteins to induce DNA bending.

In order to attempt to increase protein-induced DNA bending, we introduced reciprocal mutations into MEF2A. The double-mutant MEF2A protein K4V/E14K induces DNA bending to a greater extent than wild-type MEF2A (Fig. 8B; 19.3 ± 0.9° for wild type and 34.1 ± 1.36° for K4V/E14K). Of these two mutations, E14K plays the major role in promoting protein-induced DNA bending (Fig. 8B). These gain-of-function experiments further underscore the importance of a single amino acid, K154 (SRF) or E14 (MEF2A), as a major determinant of the ability of MADS-box transcription factors to bend DNA.

K154 (SRF) and E14 (MEF2A) are key determinants of DNA-binding specificity. The unique N terminus of SRF plays a major role in determining the differential DNA-binding specificities of SRF and MEF2A (20, 30). The introduction of the mutation K154E into an N-terminally truncated SRF derivative completes the conversion of SRF DNA-binding specificity to that of MEF2A and blocks its ability to bind to SRE-like sequences (30) (Fig. 9B; lanes 5 and 12). $core^{MEF2A}$ is unable to bind efficiently to the c-*fos* SRE (Fig. 9B, lane 8). Introduction of the double mutation K4V/E14K into MEF2A increases its ability to bind to the c-*fos* SRE (Fig. 9B, lane 10). Of these two mutations, E14K is sufficient to confer this increased SRE binding (Fig. 9B; compare lanes 9 and 11). All of these mutant MEF2A proteins still efficiently bind the N10 site (Fig. 9B, lanes 1 to 4). In order to more precisely define this change in DNA-binding specificity, we used a competition assay and compared the ability of the M1 site to act as a competitor for N10 binding. This mutant N10 site is identical to the M1 site but differs at just two symmetrical positions and converts it into an SRE-like site (Fig. 9C). The M1 site binds $core^{MEF2A}$ very poorly (23) and competes poorly with $core^{MEF2A}$ binding to the N10 site (Fig. 9D and E). However, the M1 site competes better with $core^{MEF2A}$ (E14K) than wild-type $core^{MEF2A}$ for binding to the N10 site (Fig. 9D and E), thereby demonstrating an increased affinity for this site. The E14K mutation, therefore, allows MEF2A to recognize SRE-like sequences and in particular allows it to recognize palindromically oriented C:G base pairs at the ±4 position in the binding site. These results, therefore, demonstrate a role for the residues K154 (SRF) and E14 (MEF2A) in determining the unique DNA-binding specificities of these two transcription factors. Moreover, these same two residues play a key role in mediating the differential DNA-bending properties of SRF and MEF2A, suggesting a link between protein-induced DNA bending and DNA-binding specificity.

DISCUSSION

Members of the MADS-box transcription factor family exhibit significant sequence similarity within their DNA-binding domains. It might be predicted that the nonconserved amino acids would confer different properties on individual transcription factors, whereas conserved amino acids would confer sim-

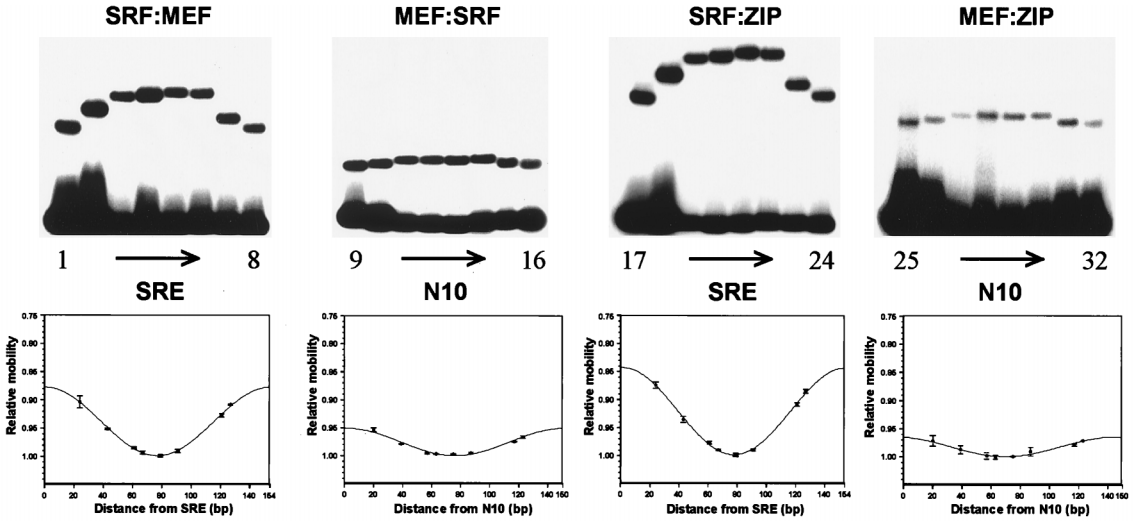

FIG. 6. Differential DNA bending of SRF and MEF2A is mediated by their MADS boxes. Circular permutation analysis of chimeric SRF and MEF2A complexes with the c-*fos* SRE and N10 sites. SRF:MEF, MEF:SRF, SRF:ZIP, and MEF:ZIP were bound to each of the circularly permuted probes containing either the c-*fos* SRE (lanes 1 to 8 and 17 to 24) or the N10 site (lanes 9 to 16 and 25 to 32). The following probes (see legend to Fig. 4) were used: M1 (lanes 1, 9, 17, and 25), Bg (lanes 2, 10, 18, and 26), Xh (lanes 3, 11, 19, and 27), EV (lanes 4, 12, 20, and 28), Sm (lanes 5, 13, 21, and 29), St (lanes 6, 14, 22, and 30), Rs (lanes 7, 15, 23, and 31), and BH (lanes 8, 16, 24, and 32). The data from each circular permutation experiment are shown graphically beneath each set of primary data and were quantified as described in the legend to Fig. 4.

ilar functional and structural properties. Indeed, nonconserved residues located in the recognition helix and N terminal to the MADS box of SRF confer a DNA-binding specificity related to but distinct from that exhibited by members of the MEF2 subfamily (20, 30). In the present study, we have dissected the DNA-binding mechanisms used by the SRF and MEF2 subfamily of MADS-box transcription factors and find that they differ in several key aspects. The major difference is that in

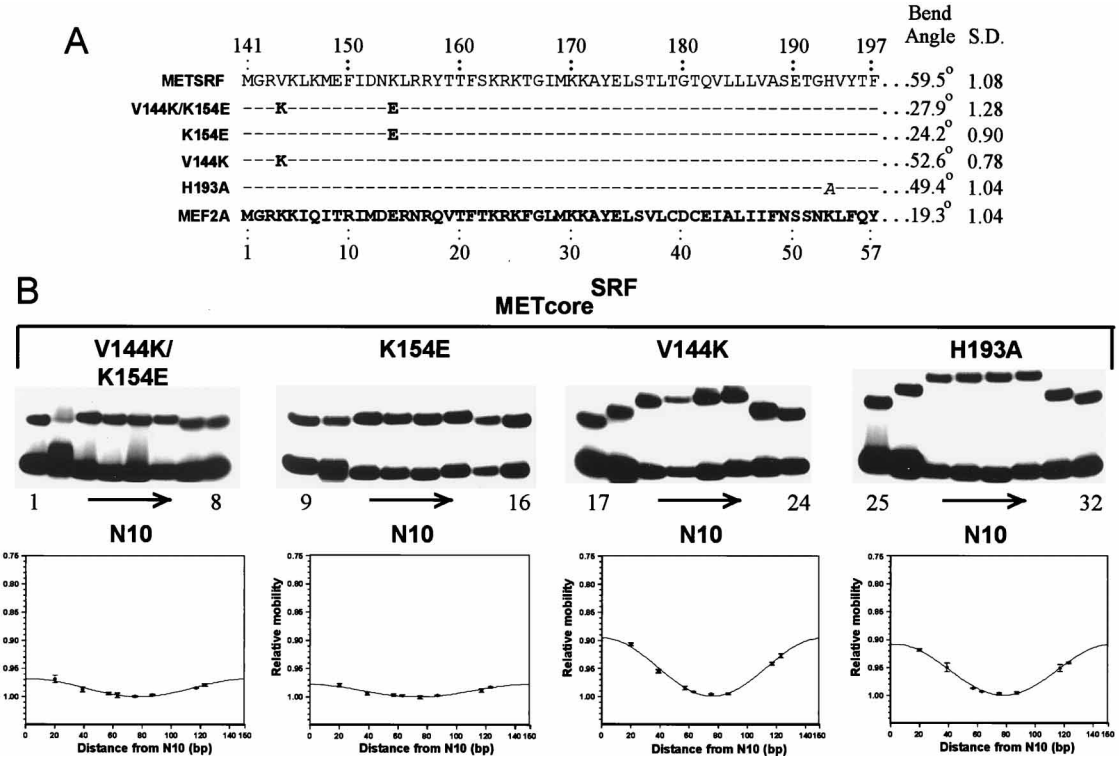

FIG. 7. Mapping the amino acid(s) which determines the differential DNA bending induced by SRF and MEF2A. (A) Sequences of the N-terminal ends of METcore^{SRF} and MEF2A (boldface) DNA-binding domains. The numbers above and below these sequences refer to SRF and MEF2A amino acid residues, respectively. The residues altered in METcore^{SRF} in each mutant protein are indicated between these sequences. DNA-bending angles were calculated from the data in panel B. SD, standard deviations ($n - 1$). (B) Circular permutation analysis of mutant METcore^{SRF} proteins bound to the N10 site. The following probes (see legend to Fig. 4) were used: M1 (lanes 1, 9, 17, and 25), Bg (lanes 2, 10, 18, and 26), Xh (lanes 3, 11, 19, and 27), EV (lanes 4, 12, 20, and 28), Sm (lanes 5, 13, 21, and 29), St (lanes 6, 14, 22, and 30), Rs (lanes 7, 15, 23, and 31), and BH (lanes 8, 16, 24, and 32). The data from each circular permutation experiment are shown graphically beneath each set of primary data and were quantified as described in the legend to Fig. 4.

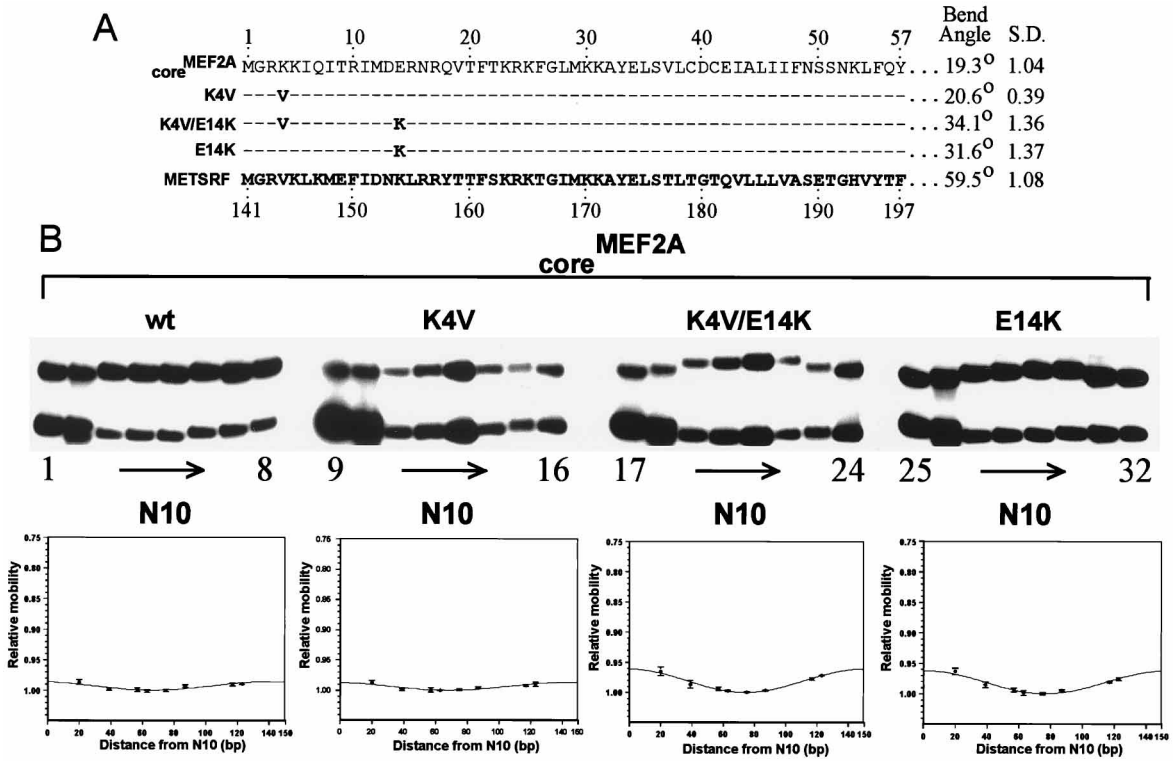

FIG. 8. Gain-of-function MEF2A mutants induce DNA bending. (A) Sequences of the N-terminal ends of MEF2A and METcore^{SRF} (boldface) DNA-binding domains. The numbers above and below these sequences refer to full-length MEF2A and SRF amino acid residues, respectively. The residues altered in core^{MEF2A} in each mutant protein are indicated between these sequences. DNA-bending angles were calculated from the data in panel B. SD, standard deviations ($n - 1$). (B) Circular permutation analysis of wild-type and mutant core^{MEF2A} proteins bound to the N10 site. The following probes (see the legend to Fig. 4) were used: M1 (lanes 1, 9, 17, and 25), Bg (lanes 2, 10, 18, and 26), Xh (lanes 3, 11, 19, and 27), EV (lanes 4, 12, 20, and 28), Sm (lanes 5, 13, 21, and 29), St (lanes 6, 14, 22, and 30), Rs (lanes 7, 15, 23, and 31), and BH (lanes 8, 16, 24, and 32). The data from each circular permutation experiment are shown graphically beneath each set of primary data and are quantified as described in the legend to Fig. 4.

contrast to SRF, MEF2A mediates minimal DNA distortion. Nonconserved residues within the MADS box are responsible for dictating differential DNA bending by these transcription factors. These residues also play a key role in DNA-binding specificity determination. Moreover, different basic residues play critical roles in DNA bending by SRF and MEF2A. Dimerization is a prerequisite for DNA binding and is mediated by residues located within both the MADS box and the nonconserved C-terminal extension. Although both are essential for efficient DNA binding, the roles of these C-terminal extensions in dimerization differ between MEF2A and SRF.

The role of residues in the recognition helix in DNA binding. In SRF, three basic residues, R157, K163, and R164, play critical roles in DNA binding. Conservative mutations at these positions severely compromise DNA binding (29). In the DNA-bound SRF structure (21), K163 makes base contacts in the major groove to the two guanine residues at each side of the SRF-binding site (CC[A/T]$_6$GG). R164 plays a dual role in contacting DNA (via the phosphate backbone) and dimerization, whereas R157 appears not to contact DNA. In contrast, R157 interacts with the β-loop at the C terminus of the MADS box and plays an additional role in orienting the region located N terminally to the DNA-binding α-helix (21). In MEF2A, the basic residues K23 and R24 (analogous to K163 and R164 in SRF) play important roles in DNA binding. This is also true of these residues in MEF2C (18). This suggests that in the MEF2 proteins, K23 and R24 may have functions similar to those of the analogous residues in SRF. In the case of K23, the less-severe effects of mutations on DNA binding in MEF2 may be explained by the observation that only one guanine residue is present at each side of its binding site (CTA[A/T]$_4$TAG) and hence that only one base contact is likely to be disrupted, compared to two in SRF. In contrast, R17 (in MEF2) and R157 (in SRF) play distinct roles in the two proteins, since mutations of R17 do not affect DNA binding by MEF2. This may reflect that the N-terminal extension to the DNA-binding α-helix adopts a novel orientation and/or that contacts with the β-loop are not critical for efficient DNA binding by MEF2. The former possibility is supported by the observation that residues in this N-terminal extension contribute to differential DNA-binding specificity determinations (20, 30). Moreover, since residues in the β-loop may play roles in mediating SRF-induced DNA bending (21) (Fig. 7), the lack of bending observed in MEF2A-DNA complexes may partly reflect the absence of interactions between the β-loop and R17 which may be a prerequisite to allow DNA contacts to be made between residues in the β-loop and DNA.

The mutation of other residues (Q18, T20, and K25) in the putative recognition α-helix of MEF2A has only a minor effect on DNA binding. Similarly, the mutation of K25 in MEF2C has only a minor effect on DNA binding (18). In SRF, T160 and K165 also appear to play relatively unimportant roles in DNA binding (29), although both make phosphate backbone contacts and, in the case of K165, also contribute to dimerization (21).

Taken together, these results indicate that the majority of residues conserved between SRF and MEF2A within the putative recognition α-helix play similar roles in DNA binding. However, R17/R157 is an important exception to this rule and

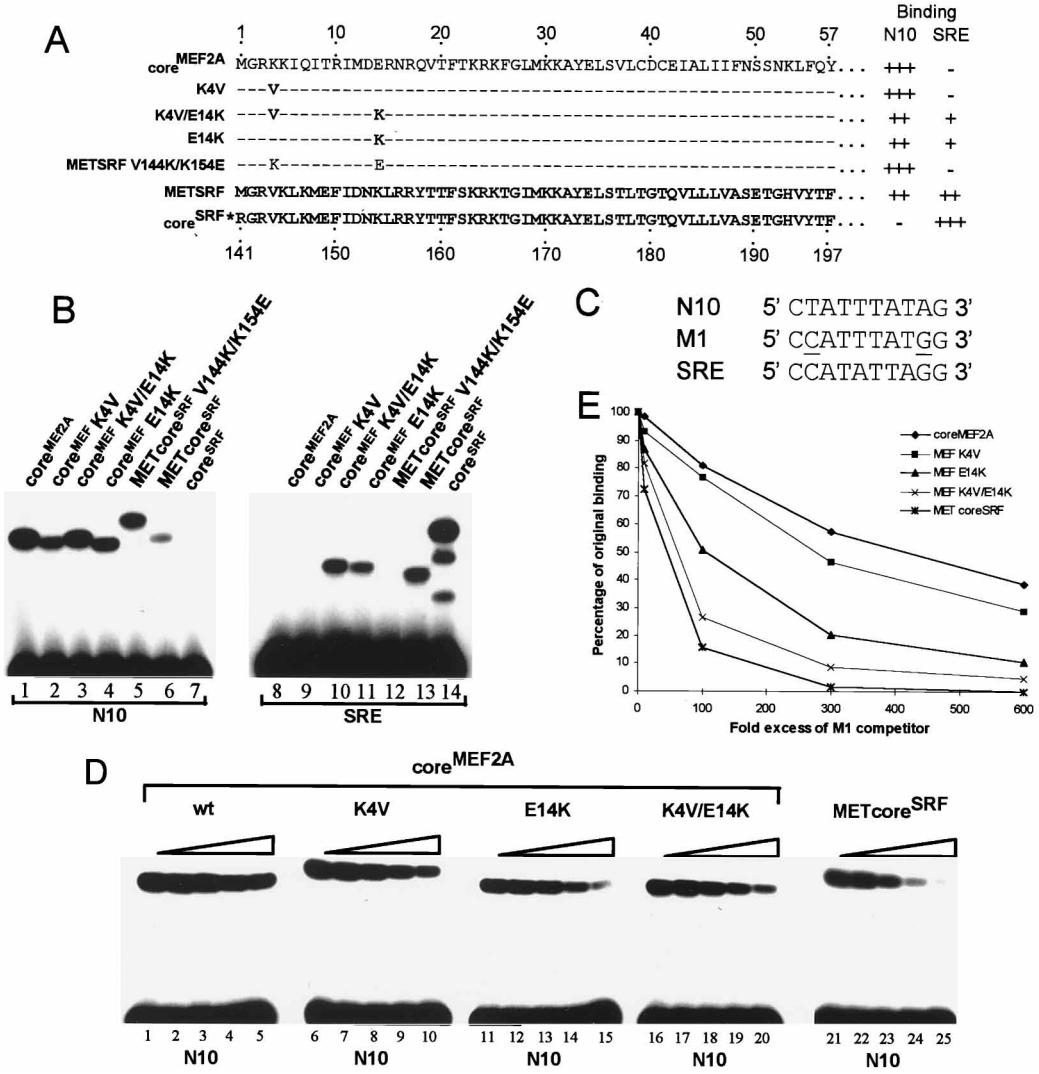

FIG. 9. K154 (SRF) and E14 (MEF2A) are key determinants of DNA-binding specificity. (A) Sequences of the N-terminal ends of MEF2A and SRF (boldface) DNA-binding domains. The numbers above and below these sequences refer to MEF2A and SRF amino acids, respectively. The asterisk preceding the core^{SRF} sequences indicates the presence of a further 10 N-terminal residues in this protein. The residues altered in core^{MEF2A} and METcore^{SRF} mutant proteins are indicated between these sequences in boldface and normal type, respectively. Binding affinities relative to wild-type core^{MEF2A} on the N10 site or core^{SRF} on the c-*fos* SRE are indicated. +++, >65%; ++, 10 to 65%; +, 1 to 10%; −, not detectable. (B) Gel retardation analysis of wild-type and mutant MEF2A and SRF DNA-binding domains to the N10 (lanes 1 to 7) and SRE (lanes 8 to 14) binding sites. Equal quantities of each protein were used in binding to the N10 site (lanes 1 to 7). However, in comparison to SRF derivatives, increased amounts of mutant and wild-type core^{MEF2A} proteins were used in binding to the c-*fos* SRE due to their lower binding affinities for this site (lanes 8 to 11, 5×-higher protein concentration than that in lanes 5 to 7). (C) Sequences of the central 10-bp motifs of the N10, M1, and SRE binding sites. Residues mutated in the N10 site to create the M1 site are underlined. (D) Competition assay by gel retardation analysis to analyze the relative affinities of mutant core^{MEF2A} proteins for the M1 site. Complexes were found between METcore^{SRF} or wild-type and mutant core^{MEF2A} proteins and the N10 site in the presence of increasing molar excesses of unlabelled M1 binding sites. Increases in the concentrations of the competitor M1 site are represented schematically above each set of lanes. The following excesses of competitor DNA were added: none (lanes 1, 6, 11, 16, and 21), 10× (lanes 2, 7, 12, 17, and 22), 100× (lanes 3, 8, 13, 18, and 23), 300× (lanes 4, 9, 14, 19, and 24), and 600× (lanes 5, 10, 15, 20, and 25). The data are representative of three independent experiments. (E) Graphical representation of the data in panel D. wt, wild type.

is indicative of an important divergence in how these transcription factors bind to DNA.

Dimerization of MADS-box proteins. Dimerization of MADS-box proteins is a prerequisite for DNA binding. Minimal DNA-binding domains are composed of the MADS-box homology region and a 20- to 30-amino-acid C-terminal extension. In the case of SRF, both biochemical data (this study) and structural data (21) indicate that residues in both the MADS box and the C-terminal extension form the dimerization interface. In contrast, in the case of MEF2A, the C-terminal extension (the MEF2 domain) does not appear to act as the major dimerization interface but is necessary for efficient dimer formation. Instead, the MADS box appears to be the major dimerization determinant. This is consistent with the conclusions derived from an alternative experimental approach regarding the highly related MEF2C transcription factor (18). Moreover, regions within and C terminal to the MADS box play different roles in the dimerization of individual *Arabidopsis* proteins. In the case of AG, the MADS box plays a major role in dimerization specificity, whereas in AP3, the major determinants are in the C-terminal extension (25). Subfamilies of MADS-box proteins, therefore, have adopted distinct dimerization mechanisms to ensure correct partner binding.

The C-terminal extension on both SRF and MEF2A can be

replaced by a leucine zipper dimerization motif to produce functional sequence-specific DNA-binding proteins. This clearly demonstrates that the contribution to dimerization mediated by the MADS-box domain is sufficient to correctly align the DNA-binding α-helices to make contact with their binding sites. Therefore, it appears that dimerization within the MADS boxes of SRF and MEF2A occurs via a similar mechanism (between two hydrophobic β-sheets and a coiled-coil interaction at the C termini of the DNA binding α-helices); however, although the C-terminal extensions are necessary for dimerization, they play distinct roles in SRF and MEF2.

DNA-bending determinants of MADS-box transcription factors. SRF induces considerable DNA bending at its recognition site (8, 21). The *Arabidopsis* proteins AP1, AG, and PI/AP3 also bend DNA significantly (26). In contrast, MEF2A induces minimal DNA distortion. Furthermore, the yeast proteins Arg80, Rlm1, and Smp1 also show differential induction of DNA bending. Arg80 bends DNA significantly, whereas Rlm1 and Smp1 induce minimal DNA distortion (38). Thus, individual members of the MADS-box transcription factor family induce DNA-bending to different extents.

Inspection of the SRF-DNA cocrystal structure reveals several residues which may be important in mediating DNA bending. In particular, phosphate backbone contacts by residues K154/K165 (in the DNA-binding α-helix) and T191/H193 (in the β-loop) are suggested to play a role in pulling the DNA into a bent confirmation (Fig. 10) (21). Of these residues, only K165 is conserved in MEF2A. Site-directed mutagenesis demonstrates that K154 and E14 play the major roles in mediating differential DNA bending induced by SRF and MEF2A, respectively. In SRF, mutations in the β-loop residues also affect DNA binding, albeit to a lesser extent. The dramatic loss of bending caused by the K154E mutation in SRF can be attributed not only to the loss of a phosphate backbone contact but also to the probable repulsion effect of introducing a negative charge at this position. Indeed, it is also likely that protein-DNA interactions mediated by other amino acids in the vicinity of K154 (R156, T191, and H193) will also be affected by this mutation. Moreover, in conjunction with the unique N terminus of SRF, K154 contributes to the difference in DNA-binding specificities between SRF and MEF2A (20, 30), and mutations at this residue also appear to affect interactions with the TCF transcription factors (30). K154, therefore, plays a pivotal role in the molecular interactions that involve SRF.

DNA bending and DNA-binding specificity. The unique N terminus of SRF plays a major role in determining its DNA-binding specificity. However, K154 within the recognition α-helix plays a role in specificity determination in addition to its role in mediating DNA bending. Moreover, the analogous residue in MEF2A, E14, plays a similar dual role in modulating its DNA-binding specificity and ability to induce DNA bending. This raises the possibility that a link exists between DNA bending and specificity determination. Such recognition is referred to as indirect readout rather than the direct protein-DNA recognition associated with the specific interactions with DNA bases. In the case of SRF, it has previously been proposed that the ability of SRF to induce DNA bending may be a major determinant of its DNA-binding specificity (21, 31). A direct correlation exists between the degrees of DNA bending exhibited by SRF and MEF2 and their abilities to interact with their cognate binding sites (Fig. 11). In particular, bending correlates with the stringency of DNA binding. High DNA bending allows recognition of SRF target sequences ($CC[A/T]_6GG$), whereas low DNA bending correlates with MEF2-like binding properties and nonrecognition of SRF-binding sites.

In addition to its role in modulating DNA bending, K154/E14, in conjunction with residues located N terminally, may also cause a reorientation of the DNA-binding α-helix which may contribute to this differential binding specificity. Such a scenario is consistent with the differential use of residues in the DNA-binding α-helix in MEF2A and MEF2C. Structural studies of MEF2 and the mutant SRF-DNA complexes are required to help unravel the connections between DNA bending and DNA-binding specificity determinations.

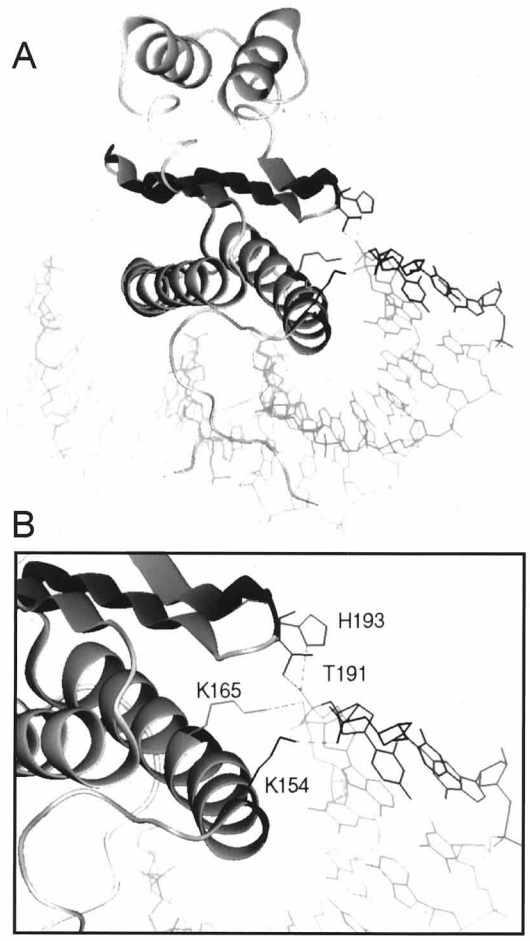

FIG. 10. DNA-protein contacts in the vicinity of K154. The DNA-binding domain of SRF bound to DNA (A) (21) is enlarged (B) to illustrate four residues which form hydrogen bonds (dashed lines) with the sugar-phosphate DNA backbone. K154 and K165 are found within the DNA-binding α-helix, while T191 and H193 are found within the β-loop.

Role of differential DNA bending in MADS-box protein function. Many transcriptional regulatory proteins bend DNA upon binding. Notable examples include TBP (14), CAP (27), bZIP proteins (11, 12), SRY (24), and E2F (4). However, it is unclear what role protein-induced DNA bending plays in transcriptional regulation, although it has been proposed to serve an architectural role in determining promoter structure (reviewed in reference 37). In the case of SRF, interaction with TCF transcription factors causes a change in protein-induced DNA bending, thereby suggesting a role of DNA bending in modulating transcription factor complex assembly (31). Indeed, the mutation K154E severely affects SRF-induced DNA bending and appears to disrupt ternary complex function with TCFs and the SRE (30). In comparison to SRF, MEF2A induces greatly reduced DNA bending. Therefore, it is expected that the architecture of MEF2-containing promoter complexes

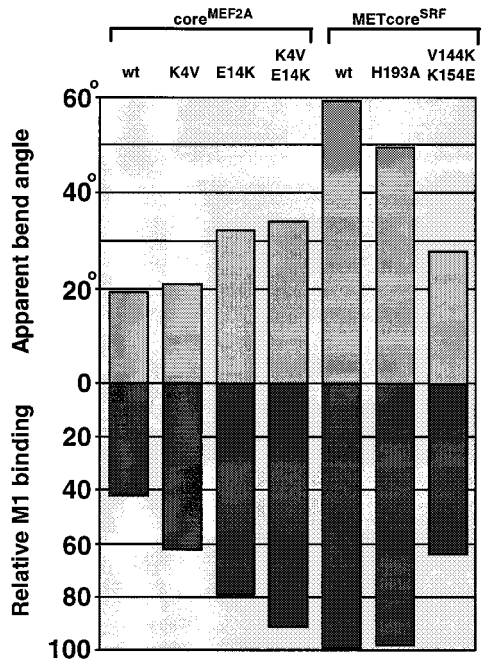

FIG. 11. Increased induction of DNA bending correlates with increased SRE-like site binding. The apparent angles of DNA bending induced by wild-type (wt) and mutant SRF and MEF2A derivatives and relative binding to the SRE-like M1 site (indicated by percentage of competition of N10 binding at a 300-fold molar excess of the M1 competitor [Fig. 9E] [38]) are shown as shaded and dark bars, respectively. An increase in ability to bend DNA correlates with the increased ability to bind to the M1 site.

would differ significantly from those containing SRF. Interfaces exposed for interaction with accessory factors and the relative positions of DNA-bound coregulatory partners are likely to differ considerably. Myogenic basic helix-loop-helix proteins represent such coregulatory partners (10, 17). Thus, differential DNA-bending properties of individual members of the MADS-box transcription factors are likely to contribute to both the DNA-binding specificity and multicomponent nucleoprotein complex formation on target promoters.

ACKNOWLEDGMENTS

We thank Margaret Bell for excellent technical assistance and Catherine Pyle for excellent secretarial assistance. We also thank Bob Liddell for oligonucleotide synthesis and DNA sequencing. We are grateful to Janet Quinn and to members of our laboratory for helpful discussions and comments on the manuscript. We are grateful to Jason Kahn for advice and to Ian Cowell for advice and reagents.

This work was supported by the Royal Society, the Nuffield Foundation, the North of England Cancer Research Campaign, and an MRC studentship to Adam West.

REFERENCES

1. **Breitbart, R. E., C.-S. Liang, L. B. Smoot, D. A. Laheru, V. Mahdavi, and B. Nadal-Ginard.** 1993. A fourth human MEF2 transcription factor, hMEF2D, is an early marker of the myogenic lineage. Development **118:**1095–1106.
1a. **Brown, A. L., and A. D. Sharrocks.** Unpublished data.
2. **Buckingham, M.** 1994. Molecular biology of muscle development. Cell **78:** 15–21.
3. **Cowell, I. G., A. Skinner, and H. C. Hurst.** 1992. Transcriptional repression by a novel member of the bZIP family of transcription factors. Mol. Cell. Biol. **12:**3070–3077.
4. **Cress, W. D., and J. R. Nevins.** 1996. A role for a bent DNA structure in E2F-mediated transcriptional activation. Mol. Cell. Biol. **16:**2119–2127.
5. **Derbyshire, K. M., J. J. Salvo, and N. D. F. Grindley.** 1986. A simple and efficient procedure for saturation mutagenesis using mixed oligodeoxynucleotides. Gene **46:**145–152.
6. **Dolan, J. W., and S. Fields.** 1991. Cell-type-specific transcription in yeast. Biochim. Biophys. Acta **1088:**155–169.
7. **Drak, J., and D. M. Crothers.** 1991. Helical repeat and chirality effects on DNA gel electrophoretic mobility. Proc. Natl. Acad. Sci. USA **88:**3074–3078.
8. **Gustafson, T. A., A. Taylor, and L. Kedes.** 1989. DNA bending is induced by a transcription factor that interacts with the human *c-FOS* and α-actin promoters. Proc. Natl. Acad. Sci. USA **86:**2162–2166.
9. **Kahn, J., and D. M. Crothers.** 1992. Protein-induced bending and DNA cyclisation. Proc. Natl. Acad. Sci. USA **89:**6343–6347.
10. **Kaushal, S., J. W. Schneider, B. Nadal-Ginard, and V. Mahdavi.** 1994. Activation of the myogenic lineage by MEF2A, a factor that induces and cooperates with MyoD. Science **266:**1236–1240.
11. **Kerppola, T. K., and T. Curran.** 1993. Selective DNA bending by a variety of bZIP proteins. Mol. Cell. Biol. **13:**5479–5489.
12. **Kerppola, T. K.** 1996. Fos and Jun bend the AP-1 site: effects of probe geometry on the detection of protein-induced DNA bending. Proc. Natl. Acad. Sci. USA **93:**10117–10122.
13. **Kim, J., C. Zweib, C. Wu, and S. Adhya.** 1989. Bending of DNA by gene regulatory proteins: construction and use of a DNA bending vector. Gene **85:**15–23.
14. **Kim, J. L., D. B. Nikolov, and S. K. Burley.** 1993. Co-crystal structure of TBP recognizing the minor groove of a TATA element. Nature **365:**520–527.
15. **Landt, O., H. P. Grunert, and U. Hahn.** 1990. A general method for rapid site-directed mutagenesis using the polymerase chain reaction. Gene **96:**125–128.
16. **Ma, H.** 1994. The unfolding drama of flower development: recent results from genetic and molecular analyses. Genes Dev. **8:**745–756.
17. **Molkentin, J. D., B. L. Black, J. F. Martin, and E. N. Olsen.** 1995. Cooperative activation of muscle gene expression by MEF2 and myogenic bHLH proteins. Cell **83:**1125–1136.
18. **Molkentin, J. D., B. L. Black, J. F. Martin, and E. N. Olson.** 1996. MEF2B is a potent transactivator expressed in early myogenic lineages. Mol. Cell. Biol. **16:**2627–2636.
19. **Norman, C., M. Runswick, R. Pollock, and R. Treisman.** 1988. Isolation and properties of cDNA clones encoding SRF, a transcription factor that binds to the *c-fos* serum response element. Cell **55:**989–1003.
20. **Nurrish, S. J., and R. Treisman.** 1995. DNA binding specificity determinants in MADS-box transcription factors. Mol. Cell. Biol. **15:**4076–4085.
21. **Pellegrini, L., S. Tan, and T. J. Richmond.** 1995. Structure of serum response factor core bound to DNA. Nature **376:**490–498.
22. **Pollock, R., and R. Treisman.** 1990. A sensitive method for the determination of protein-DNA binding specificities. Nucleic Acids Res. **18:**6197–6204.
23. **Pollock, R., and R. Treisman.** 1991. Human SRF-related proteins: DNA-binding properties and potential regulatory targets. Genes Dev. **5:**2327–2341.
24. **Pontiggia, A., R. Rimini, V. R. Harley, P. N. Goodfellow, R. Lovell-Badge, and M. E. Bianchi.** 1994. Sex-reversing mutations affect the architecture of SRY-DNA complexes. EMBO J. **13:**6115–6124.
25. **Riechmann, J. L., B. A. Krizek, and E. M. Meyerowitz.** 1996. Dimerisation specificity of *Arabidopsis* MADS-domain homeotic proteins APETALA1, APETALA3, PISTILLATA and AGAMOUS. Proc. Natl. Acad. Sci. USA **93:**4793–4798.
26. **Riechmann, J. L., M. Wang, and E. M. Meyerowitz.** 1996. DNA-binding properties of Arabidopsis MADS-domain homeotic proteins proteins APETALA1, APETALA3, PISTILLATA and AGAMOUS. Nucleic Acids Res. **24:**3134–3141.
27. **Schultz, S. C., G. C. Shields, and T. A. Steitz.** 1991. Crystal structure of a CAP-DNA complex: the DNA is bent by 90°. Science **253:**1001–1007.
28. **Sharrocks, A. D.** 1994. A T7 expression vector for producing N- and C-terminal fusion proteins with glutathione *S*-transferase. Gene **138:**105–108.
29. **Sharrocks, A. D., H. Gille, and P. E. Shaw.** 1993. Identification of amino acids essential for DNA binding and dimerization in $p67^{SRF}$: implications for a novel DNA-binding motif. Mol. Cell. Biol. **13:**123–132.
30. **Sharrocks, A. D., F. Von Hesler, and P. E. Shaw.** 1993. The identification of elements determining the different DNA binding specificities of the MADS-box proteins $p67^{SRF}$ and RSRFC4. Nucleic Acids Res. **21:**215–221.
31. **Sharrocks, A. D., and P. Shore.** 1995. DNA bending in the ternary nucleoprotein complex at the c-*fos* promoter. Nucleic Acids Res. **23:**2442–2449.
32. **Shaw, P. E.** 1992. Ternary complex formation over the *c-fos* serum response element: $p62^{TCF}$ exhibits dual component specificity with contacts to DNA and an extended structure in the DNA-binding domain of $p67^{SRF}$. EMBO J. **8:**3011–3019.
33. **Shore, P., and A. D. Sharrocks.** 1994. The transcription factors Elk-1 and serum response factor interact by direct protein-protein contacts mediated by a short region of Elk-1. Mol. Cell. Biol. **14:**3283–3291.
34. **Shore, P., and A. D. Sharrocks.** 1995. The MADS-box family of transcription factors. Eur. J. Biochem. **229:**1–13.
35. **Treisman, R.** 1992. The serum response element. Trends Biochem. Sci. **17:**423–426.
36. **Weigel, D., and E. M. Meyerowitz.** 1994. The ABCs of floral homeotic genes. Cell **78:**203–209.
37. **Werner, M. H., A. M. Gronenborn, and G. M. Clore.** 1996. Intercalation, DNA kinking and the control of transcription. Science **271:**778–784.
38. **West, A. E., and A. D. Sharrocks.** Unpublished data.